Nuclear Instruments and Methods in Physics Research A276 (1989) 1–7
North-Holland, Amsterdam

SHIELDING OF PROTON ACCELERATORS: A COMPARISON BETWEEN THE MOYER MODEL AND MONTE CARLO CALCULATIONS

H. DINTER and K. TESCH

Deutsches Elektronen-Synchrotron DESY, D-2000 Hamburg 52, FRG

C. YAMAGUCHI

KEK, National Laboratory for High Energy Physics, Oho 1-1, Tsukuba, Japan 305

Received 5 September 1988

The FLUKA Monte Carlo program was used to calculate the dose equivalent behind a homogeneous concrete shielding for primary energies between 10 and 800 GeV, concrete thickness between 1 and 2.3 m and various target lengths. The results do not agree with the physical basis of the Moyer model and its assertions. A suggestion for the practical estimation of the dose equivalent is given.

1. Simple dose calculations

The experimental or theoretical estimation of the dose behind an accelerator's shielding is simplest when the absorption of the primary beam shows a simple source distribution and the shielding has a simple geometry. The simplest source distributions are point sources and line sources with a constant source strength per unit length. A point source can be created by a thin target; since the greatest portion of the beam energy at high-energy accelerators is absorbed by very thick targets, this type of target can be idealised to a point source when the distance to the target is large compared to the target length. In designing shields for radiation protection purposes a thick target is nearly always assumed since it produces the highest dose. In this paper we will always consider a homogeneous wall of thickness d parallel to the beam, and assume a pointlike target.

Two further simplifications suggest themselves. One first assumes that at large angles with respect to the primary beam the dose is determined only by the most penetrating component of the secondary radiation produced in the target, and hence its attenuation is described by a single attenuation coefficient. At high-energy proton accelerators this component is considered to be neutrons with energies around 100 MeV and the low-energy neutrons in radiation equilibrium with them when passing through the shielding. Their absorption length is greater than that of the charged particles (produced at large angles) or the evaporation neutrons or giant-resonance neutrons. Secondly, one assumes that the maximum of the dose lies at an angle $\theta \approx 90°$ to the beam – in other words the intensity of the secondary radiation produced within the target and increasing from 90° to 0° is overcompensated by the increasing effective thickness of the homogeneous shielding. Thus the estimation of the dose equivalent H per primary proton is given by the simple equation:

$$H = H_0 \left(\frac{E}{E_0} \right)^{\alpha} \frac{e^{-d/\lambda_H}}{r^2}, \tag{1}$$

where E is the primary energy, d is the thickness of the wall and r the distance to the target. The parameters H_0, α, and λ_H have to be obtained experimentally or calculated; H_0 and α can depend on the target and λ_H on the primary energy.

Eq. (1) can be improved if the angular distribution of the secondaries is also taken into consideration. Experiments show that the fluence of the secondary particles from a thin target and at large angles θ are given by the term $\exp(-\beta\theta)$. Its attenuation shall be described by a single attenuation coefficient in the entire angular range considered. Thus one obtains the following equation for the dose equivalent per primary proton along a shielding wall which is parallel to and at a distance a from the beam:

$$H(z) = H_0 \left(\frac{E}{E_0} \right)^{\alpha} e^{-\beta\theta} \frac{\exp(-d/(\lambda_H \sin\theta))}{r^2}, \tag{2}$$

$$\sin\theta = \frac{a+d}{r},$$

$$z = 0 \quad \text{for } \theta = 90°.$$

Since assuming a thin target is generally unsuitable for radiation protection purposes, eq. (2) is also applied to thick targets. Eq. (2) is known as the Moyer model. It

enables the calculation of the dose along a homogeneous shielding for a target considered to be pointlike. Furthermore, it enables the calculation of the dose behind a shielding of a homogeneous line source since for this the angular distribution is required. The most important works dealing with the Moyer model are given in refs. [1–5].

Semiempirical methods such as using of eq. (1) or (2) have well proved themselves in the dimensioning of shielding, although only few experimental or theoretical results are available as a foundation. Thus – as we will show – the assumptions which led to the Moyer model have not been sufficiently checked, and the parameters in eq. (2) are not known to a desirable accuracy. Hence every possibility should be used to examine and improve the simple shielding models. We carried out such examinations with the aid of the well-known Monte Carlo program FLUKA.

2. Monte Carlo calculations

Two major difficulties are encountered when using Monte Carlo programs for calculating the dose behind a shielding. Since usually only large shielding thicknesses are of interest, the hadronic–electromagnetic cascade must be followed to considerable depths, which comes up against performance limitations of current computers. One way out is to use weighted programs such as CASIM [6]. However, for a comparison with eq. (2), we are especially interested in the lateral spread of the cascade that cannot be correctly reproduced by CASIM. Hence we chose the analogue program FLUKA [7], where we had to restrict the shielding thickness to 2.3 m of concrete – for such a shielding an IBM-3084Q computer requires 4 h computing time for dealing with a single shielding geometry.

A second problem is that very low energy particles also contribute to the dose whereas Monte Carlo programs almost always have a cutoff energy in order to save computing time. If a particle sinks below this threshold its energy is deposited locally. For our calculations the cutoff energy was set to 300 MeV/c or 50 MeV for neutrons. The dose equivalent was calculated as follows. The chosen geometry is shown in fig. 1 – it represents practical requirements. The energy deposited within the water layer is calculated with the FLUKA program and multiplied by a quality factor of 5. This value corresponds approximately to the expected neutron spectrum – it was recently confirmed experimentally behind thick shielding [8]. In the following we assume that the dose equivalent $H(z)$ along a shielding wall can be calculated in this way in spite of this cutoff energy. In our earlier work we calculated the maximum of the dose equivalent behind concrete shielding already

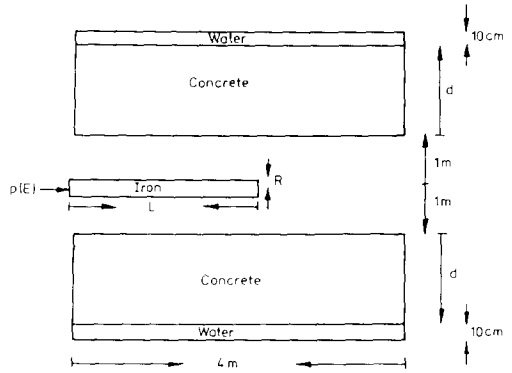

Fig. 1. Standard geometry for Monte Carlo calculations.

in this way and obtained good agreement with other experimental and theoretical results (table 1 of ref. [9]).

The calculations were carried out at DESY with the program version FLUKA82 and at KEK with the version FLUKA86. There was good agreement between both versions – averaged over numerous geometries and primary energies the differences are less than 10%.

We considered only ordinary concrete ($\rho = 2.5$ g cm^{-3}) as shielding material. The Moyer model eq. (2) is only valid for shielding material which contains hydrogen. It is not applicable for iron since in this material the low-energy neutrons (in the keV range) are more penetrating than the high-energy neutrons. The problems of iron shielding have been discussed in ref. [9].

In this report we present the calculated dose equivalent $H(z)$ along a shielding for primary energies between 10 and 800 GeV and examine which parameters are usable for eq. (2). In ref. [5] the value of the parameter α is given as 0.80 ± 0.1. This has already been confirmed by Yamaguchi [10] with the aid of the CASIM Monte Carlo program for primary energies between 3 GeV and 1 TeV, assuming a long iron target. Thus we will stick to this value for the following results. The energy E_0 is defined as 1 GeV.

3. Results and discussion of the parameter values

3.1. The parameter λ

The Moyer model assumes that the dose behind a not-too-thin shielding originates from high-energy neutrons around 100 MeV and low-energy neutrons in radiation equilibrium. Then the exponential decay of the dose can be described by a single attenuation coefficient λ_H. It is presumed that λ_H is neither dependent on the primary energy E, nor on the angle θ. The value of λ_H is given as 117 g cm^{-2} with a 2% error in ref. [4]. The original assumption of angle-independency was made by Moyer and – as far as we can ascertain – has

neither been confirmed experimentally nor theoretically. Stevenson et al. mention as confirmation in ref. [3] a shielding experiment at the Bevatron at 6.2 GeV [11]. However, here the beam was directed onto a compact block of concrete and isoflux contours were measured by threshold counters. From these data the attenuation of the flux density was determined along lines that subtend from the point of beam entry at angles from 0° to 60°. This is not the geometry of the Moyer model, furthermore the dose attenuation coefficient is required in the range 60° to 90°. An important contribution to the determination of the parameters in eq. (2) is a shielding experiment carried out at CERN (ref. [12]; see also ref. [3]); here the evaluation presupposed the angle and energy independence of λ_H.

Some evidence that contradicts the angle independency is provided by two 30 GeV experiments carried out at Brookhaven [13,14], and by calculations for a 250 MeV proton beam [15]. In the experiments the flux densities of neutrons with energies above 20 MeV were measured in sand and steel shieldings. Thin targets were used and the geometry was principally that of fig. 1. Unfortunately, in neither work an attenuation coefficient (without the $1/r^2$ dependency) is given, but one can obtain it from fig. 6 in ref. [13] and fig. 6 in ref. [14]. We have already given it for sand in fig. 2 of ref. [9] – there is a decrease (strongly scattering) from 170 to around 120 g cm^{-2} in the angular range 20° to 60°. In steel it decreases from 350 to 160 g cm^{-2} from $\theta = 15°$ to $\theta = 90°$. Dose attenuation coefficients were calculated with the programs HETC and ANISN for primary proton energies of 250 MeV by Hagan et al. [15]. Even at this low primary energy λ_H decreases from 110 g cm^{-2} for $0° < \theta < 15°$ to 79 g cm^{-2} for $90° < \theta < 180°$ (see fig. 4).

In order to study the dependency of λ_H on the angle θ and primary energy E, we calculated the dose equivalent behind four shieldings of thickness d and for five primary energies for the geometry shown in fig. 1. Most of the calculations were carried out for a thick iron target that is sufficiently long for the longitudinal development of the cascade, but has no significant side shielding effect; the cascade continues within the concrete shielding. In principle one cannot use eq. (2) to describe the angular distribution of the cascade emerging from such a target since there is no fixed source point. In order to enable an approximate comparison with eq. (2) we set – somewhat arbitrarily – the vertex of the angle θ to the point of the maximum energy deposition within the target. Fig. 2 is an example of the evaluation where the results of four calculations for 25 GeV are entered into the projection of the cylinderlike geometry so that the regions for which the doses were obtained are also visible. All the results are displayed in figs. 3a–e. The position z_E of each vertex is given in table 1. λ_H can be obtained from the four dose values

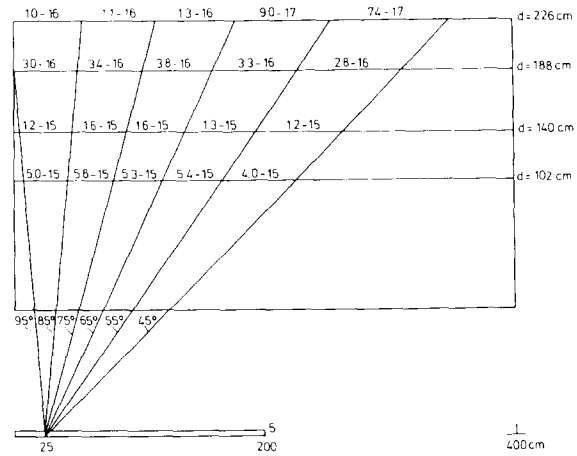

Fig. 2. Results of four calculations of the dose equivalent (in Sv per proton) for four concrete thicknesses d. The water layer behind each concrete shield is not shown. 5.0 – 15 means 5.0×10^{-15}.

for each angular range and for a given target length L, the result is shown in fig. 4.

As further information we also calculated the attenuation coefficient λ_S of the star density. Traditionally a "star" is known as the result of an inelastic interaction. The star density was determined in concrete at shielding thicknesses of 65, 100, 130, 165 and 200 cm, and from the five values the λ_S was calculated for each angular region. The results are shown in fig. 5. The vertex of the angle θ was placed within the maximum of the star density – the location z_S is also given in table 1.

Figs. 4 and 5 show no plausible dependency on E. However an angle dependency is clearly visible, it is stronger for λ_S than for λ_H. Due to the energy independence we can average the values for one angle and obtain the lines in figs. 4 and 5 and the final results in table 2.

We examined values of λ_H for $\theta > 90°$ only at 100 GeV with a slightly altered geometry from that in fig. 1. We found that λ_H did not vary in the range 90° to 120°, here we obtained values of around 100 g cm^{-2}.

Table 1
Distances of the positions of maximum energy density and maximum star density, z_E and z_S, from the beginning of the target, as a function of the primary energy E

E [GeV]	z_E [cm]	z_S [cm]
9	20	20
25	25	30
100	30	35
300	32	45
800	35	50

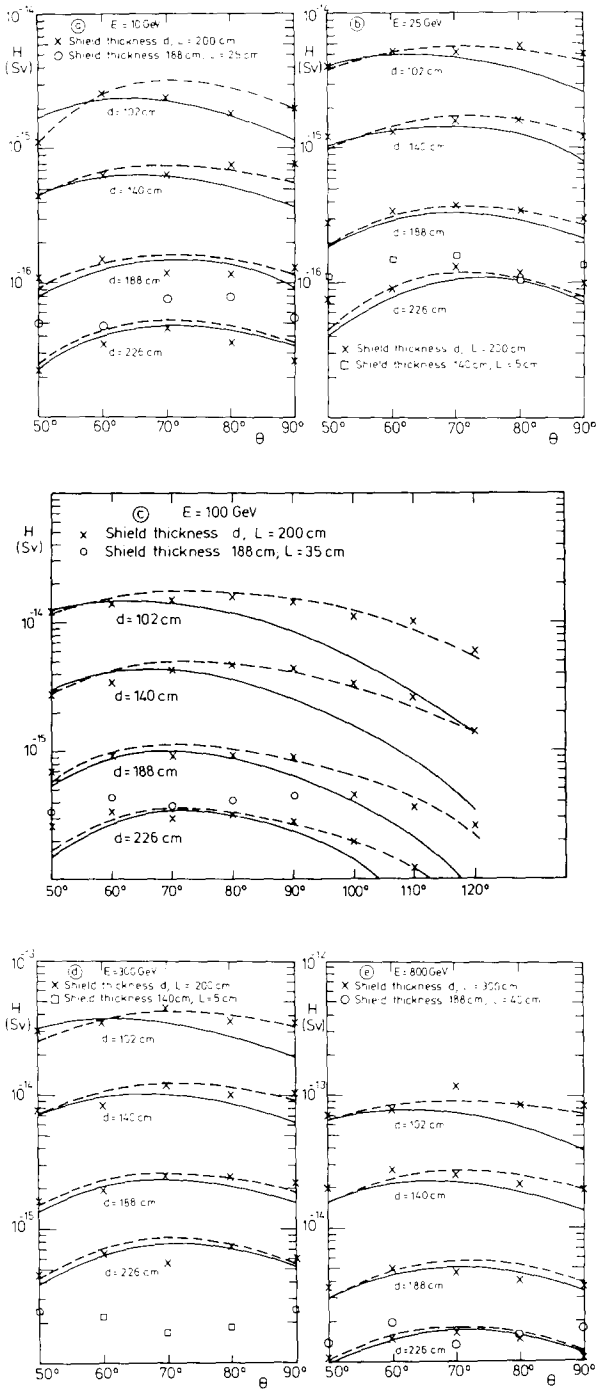

Fig. 3. The dose equivalent per proton behind concrete shielding for five primary energies E. The results of the Monte Carlo calculations are displayed as points. Radius of the iron target: $R = 5$ cm for 10 and 25 GeV, $R = 7.5$ cm for 100, 300 and 800 GeV. Continuous line: eq. (2) with $H_0 = 2.8 \times 10^{-13}$ Sv m^2, $\beta = 2.3$ rad^{-1}, and $\lambda_H = 117$ g cm^{-2}. Dashed line: eq. (2) with $H_0 = 4.2 \times 10^{-14}$ Sv m^2, $\beta = 0.5$ rad^{-1}, and λ_H from table 2.

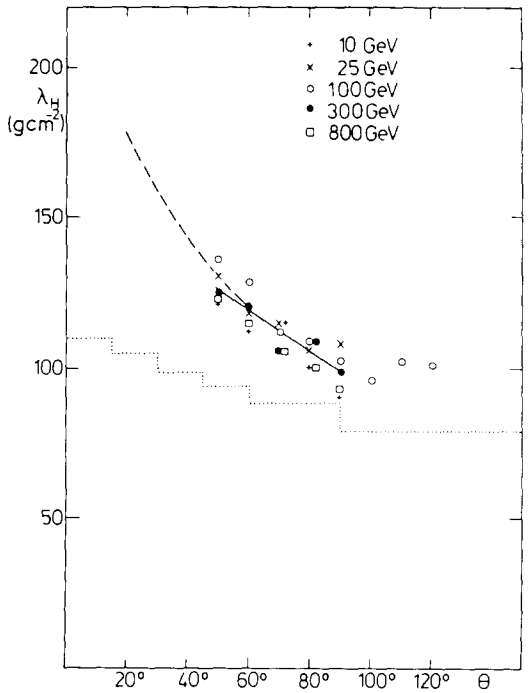

Fig. 4. The dependency of the attenuation coefficient for the dose equivalent upon the angle to the direction of the primary beam. The results of the Monte Carlo calculations are displayed as points, the continuous line is their average value in the region 50° to 90°. For comparison: The attenuation coefficient for the neutron flux density above 20 MeV at $E = 30$ GeV, from ref. [13] (dashed line); the attenuation coefficient for the dose equivalent at $E = 250$ MeV, from ref. [15] (dotted line).

These values and (for comparison) the experimental values for the flux density of neutrons above 20 MeV from ref. [13] are also shown in fig. 4. The angle dependence means that the dose behind a shielding is caused not only by a single radiation component.

We have established that the dose equivalent and the star density have differing attenuation coefficients. For the estimation of concrete shielding with Monte Carlo

Table 2
Attenuation coefficients in concrete for the dose equivalent and for the star density, λ_H and λ_S, as a function of the angle θ. The last column contains values of k for the equation $H = kS$

θ [deg]	λ_H [g cm^{-2}]	λ_S [g cm^{-2}]	k [Sv cm^3]
50	126	141	1.4×10^{-7}
60	119	131	9.7×10^{-8}
70	112	121	7.7×10^{-8}
80	105	112	6.6×10^{-8}
90	99	104	5.4×10^{-8}

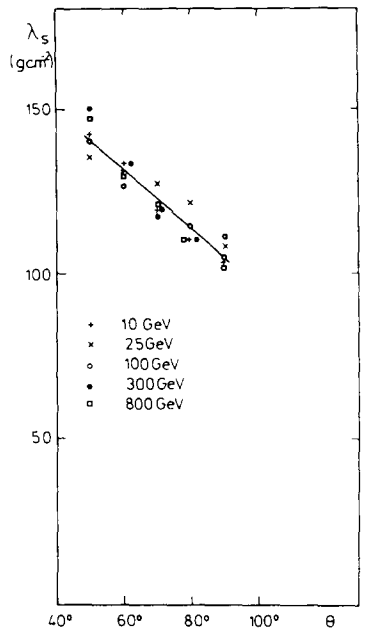

Fig. 5. The dependency of the attenuation coefficient for the star density upon the angle to the direction of the primary beam. The results of the Monte Carlo calculations are displayed as points, the straight line is their average value.

calculations a proportionality is often assumed between both quantities: $H = kS$. Apparently k is not constant within a shielding. However, we found that k is almost independent of the impinging energy and the shielding thickness (up to our maximum value of 2.3 m) and hence we can average on these magnitudes. The resulting values of k – dependent on θ – are listed in table 2; they are valid for the star densities calculated with FLUKA.

3.2. The parameter β

The most important experimental determinations of β are collected together in ref. [3]. In some of the listed experiments the angular distribution of the dose was measured behind the shielding of thin targets (length < 1 absorption length). In the fully described CERN experiment the source are the secondaries produced by a very thin target in the synchrotron, which partly generated the hadronic cascade in the accelerator's structure behind the target. In this poorly defined line source every point is assigned the same angular distribution $\exp(-\beta\theta)$. From all these experiments a mean value of $\beta = 2.3$ rad^{-1} is extracted with an error of 5% for the angular range 60° to 120°. This value is in agreement with the angular distribution of the secondaries from a thin target, i.e. before passing through the shielding material.

Since one must assume thick targets when dimensioning shielding, most of the calculations presented in fig. 3 were carried out for very long iron targets. It is apparent that the dose is only weakly dependent on the angle θ (as defined above) – a maximum is scarcely visible. One could argue that a different angular distribution occurs for a short target, furthermore the angle θ is more clearly defined. For this reason we carried out further calculations for a concrete thickness $d = 188$ cm and target length $L = z_E + 5$ cm, where z_E is the position of the maximum energy deposition within the iron (see table 1). The vertex of the angle θ lies at $\frac{2}{3}L$. In order to maintain clarity the results have only been entered into figs. 3a, c and e. Further calculations were performed for $L = 5$ cm iron and $d = 140$ cm (greater shielding thickness could not be reached due to the time required for computation), the results are shown in figs. 3b and d. In all cases one observes a similar distribution which is only weakly dependent upon θ; within the statistical limits achieved there is no recognisable dependency of the dose distribution on the target length.

We will now only consider the results for very long targets since their statistical accuracy is better. In figs. 3a, c, and e the dose values from the Moyer model are entered with the most recent parameters from ref. [4]: $H_0 = 2.8 \times 10^{-13}$ Sv m^2; $E_0 = 1$ GeV; $\beta = 2.3$ rad^{-1} and $\lambda_H = 117$ g cm^{-2}. Satisfactory agreement is obtained with the FLUKA results for the angular range $\theta = 50°$ to 90°. However, a constant value $\lambda_H = 117$ g cm^{-2} contradicts the Monte Carlo calculations – experimental observations do not lead us to expect it either (see above). If $\lambda_H = 117$ g cm^{-2} is substituted by the λ_H values from table 2 one obtains no agreement with our calculations. Agreement is obtained for all primary energies and shielding thicknesses if one uses λ_H from table 2 and selects $\beta = 0.5$ rad^{-1} and $H_0 = 4.2 \times 10^{-14}$ Sv m^2, these curves are shown in figs. 3b and 3d. This is a purely mathematical fit – we do not believe that a physical meaning can be attributed to the $e^{(-0.5\theta)}$ term.

The angular region $\theta > 90°$ was only investigated at 100 GeV, for which the geometry was slightly altered from that in fig. 1. The results are given in fig. 3c. The set of parameters from ref. [4] gives no satisfactory agreement for $\theta > 90°$ whilst agreement remains with the above mentioned fit.

3.3. The parameter H_0

It is clear that the parameter H_0 must be strongly dependent upon the target length – we have already seen this in fig. 3. The value is given as 2.8×10^{-13} Sv m^2 with an error of 5% in ref. [4], a corresponding target length is not mentioned. A value for H_0 was obtained in ref. [3] from measurements with thin targets. The contribution of the CERN experiment was also

allowed for in ref. [3]. As mentioned above, this experiment suffered from a poorly defined target geometry. The measurements within the shielding of the proton synchrotron were evaluated using 7 free parameters. The value for H_0 depended strongly upon a correction due to the iron magnets in the synchrotron. It is not clear which target length is applicable here for the parameter H_0.

It is somewhat surprising that the value for H_0 determined in this way agrees with the dose values calculated with FLUKA for the angular region $\theta = 50°$ to $90°$ (see above), despite the fact that very long targets were employed. The dose maximum is also in agreement with measurements behind the shielding of beam absorbers at 350 and 800 GeV and with the calulations performed by O'Brien in which the production of the maximum number of stars in the iron target is assumed (cf. ref. [9]).

Since the dependency of the dose outside the shielding upon the length of the target has also practical implications, we now summarise the results of these and earlier calculations: We express the lengths of iron and aluminium targets in absorption lengths (iron = 17.1 cm, aluminium = 37.2 cm). We only consider the dose maximum along a given shielding. We remove the dependence upon the shielding thickness d and the primary energy E by normalising to the dose value which we obtain from our previous work (ref. [9], eq. (7)). One then obtains fig. 6. The individual points are scattered appreciably – the recognisable trend is sketched as a curve. The dose varies by one order of magnitude between 0.5 and 5 absorption lengths, rather independent of the primary energy.

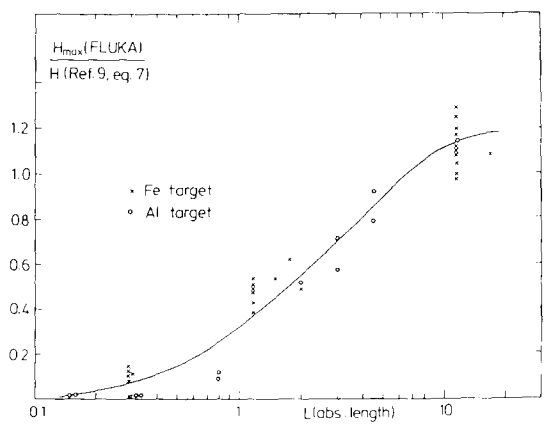

Fig. 6. The maximum dose equivalent behind a concrete shielding from Monte Carlo calculations, divided by the dose equivalent obtained with eq. (7) from ref. [9]. The points are the results of calculations for shielding thicknesses between 1 and 2.3 m and for primary energies between 10 and 800 GeV.

4. Summary and conclusions

We have calculated the dose equivalent behind concrete shielding with the FLUKA Monte Carlo program. We assumed here that the dose can be obtained from the energy deposition in a a layer of water even when the cutoff energy of the program is 50 MeV for neutrons. We used a quality factor of 5 – this value has been confirmed experimentally. It is meant to be independent of the geometry and incident energy. We restricted ourselves to the geometry shown in fig. 1 and to concrete shielding of thicknesses not larger than 2.3 m on grounds of computer time. The statistical fluctuations are not small; the results in fig. 3 are not smoothed so that one can estimate the statistical accuracy from the scattering of the points.

The results obtained with these assumptions and restrictions have been compared with eq. (2) of the Moyer model. The results are:

(a) The attenuation coefficient of the dose equivalent λ_H is not a constant for $\theta < 90°$. It decreases from 130 to 100 g cm^{-2} in the region 50° to 90° and was found to remain at 100 g cm^{-2} from 90° to 120°. The trend is in agreement with experimental results from Brookhaven. This result means that for $\theta < 90°$ the dose equivalent is caused not only by a single radiation component (viz. the neutrons with energies around 100 MeV), in contrast to the basic idea of the Moyer model.

(b) The parameter set $H_0 = 2.8 \times 10^{-13}$ Sv m^2, $\beta = 2.3$ rad^{-1}, $\lambda = 117$ g cm^{-2} and eq. (2) are in agreement for $\theta = 50°$ to 90° and long targets in which the hadronic cascade can develop longitudinally, despite the fact that $\beta = 2.3$ rad^{-1} was determined by experiments with thin targets and λ_H is not a constant for this angular region. The strong dependency upon the target thickness (fig. 6) is not taken into consideration, for thin targets H_0 is much smaller than the given value.

(c) One can fit all the results of our calculations with eq. (2) when θ-dependent λ_H values from table 2 and $H_0 = 4.2 \times 10^{-14}$ Sv m^2 and $\beta = 0.5$ rad^{-1} are used as parameters. However, we do not believe that a physical meaning can be attributed to the β term. The angular distribution of the secondary radiation measured around a thin target cannot be applied in a simple way to the dose distribution behind a concrete wall shielding a thick target. The development of the hadronic–electromagnetic cascade in the target and in the shielding takes place between both phenomena.

We conclude that the Moyer model is only an algorithm which enables experimental and theoretical data to be fitted. This point of view was also discussed in ref. [16]. If one attributes a physical meaning to the known parameters, inconsistencies are obtained. Hence the Moyer model gives no insight into the physical processes which take place within the target and the

shielding. Analytical methods or use of analog Monte Carlo programs are required for this.

If the parameter λ_H depends significantly on the angle θ, the dose behind a homogeneous shielding of a homogeneous line source cannot be calculated by means of the Moyer integrals [1].

Fortunately these statements have in practice no special consequences for calculations of shielding for simple target geometries. A line source is rarely assumed when dimensioning shielding. Usually a thick target is regarded as being nearly pointlike and the shielding thickness is determined by the maximum dose that emerges. As we have seen, the dose maximum in the range 50° to 90° is not very pronounced for all primary energies – it is a factor ≈ 1.5 greater than the dose at 90°. Thus the difference is much smaller than, e.g., the error in the assumption over the number of primary protons absorbed within the target (over long periods). Furthermore, it is usually irrelevant whether this (weakly pronounced) maximum appears at 90° to the target or a few metres downstream. If one is only interested in the dose maximum at around 90° the Moyer model eq. (2) is not necessary – the simple eq. (1) suffices. We showed in our earlier work [9] that with the parameters $H_0 = 1.5 \times 10^{-14}$ Sv m^2, $E_0 = 1$ GeV, $\alpha = 0.8$ and $\lambda_H = 107$ g cm^{-2}, eq. (1) produces sufficient agreement with the relevant shielding experiments and calculations in the range 1 GeV to 1 TeV and for targets in which the hadronic cascade can develop longitudinally.

References

[1] J.T. Routti and R.H. Thomas, Nucl. Instr. and Meth. 76 (1969) 157.

[2] J.T. Routti and M.H. Van de Voorde, Nucl. Eng. Design 21 (1972) 421.

[3] G.R. Stevenson, Liu Kuei-Lin and R.H. Thomas, Health Phys. 43 (1982) 13.

[4] J.B. McCaslin, W.P. Swanson and R.H. Thomas, Nucl. Instr. and Meth. A256 (1987) 418.

[5] R.H. Thomas and S.V. Thomas, Health Phys. 46 (1984) 954.

[6] A. Van Ginneken, Fermi National Accelerator Laboratory Report FN-272 (1975).

[7] P.A. Aarnio, J. Ranft and G.R. Stevenson, CERN Report TIS-RP/106 (1983);
P.A. Aarnio, A. Fasso, H.-J. Moehring, J. Ranft and G.R. Stevenson, CERN Report TIS-RP/168 (1986).

[8] J.D. Cossairt, Proc. 20th Midyear Topical Symp. of the Health Physics Society, Reno (1987).

[9] K. Tesch and H. Dinter, Radiat. Prot. Dos. 15 (1986) 89.

[10] C. Yamaguchi, Health Phys. 51 (1986) 812.

[11] A.R. Smith, Proc. USAEC 1st. Symp. on Accelerator Radiation Dosimetry and Experience, Brookhaven (1965).

[12] W.S. Gilbert, D. Keefe, J.B. McCaslin, H.W. Patterson, A.R. Smith, L.D. Stephens, K.B. Shaw, G.R. Stevenson, R.H. Thomas, R.D. Fortune and K. Goebel, Lawrence Radiation Laboratory UCRL-17941 (1968).

[13] W.R. Casey, C.H. Distenfeld, G.S. Levine, W.H. Moore and L.W. Smith, Nucl. Instr. and Meth. 55 (1967) 253.

[14] G.W. Bennett, G.S. Levine, H.W. Foelsche and T.E. Toohig, Nucl. Instr. and Meth. 118 (1974) 149.

[15] W.K. Hagan, B.L. Colborn, T.W. Armstrong and M. Allen, Nucl. Sci. Eng. 98 (1988) 272.

[16] R.H. Thomas, Health Phys. 53 (1987) 425.